Chemical Engineering Journal 431 (2022) 133380

Contents lists available at ScienceDirect

Chemical Engineering Journal

journal homepage: www.elsevier.com/locate/cej

Induction heating as an alternative electrified heating method for carbon capture process

Mohsen Gholami, Brieuc Verougstraete, Raphaël Vanoudenhoven, Gino V. Baron, Tom Van Assche, Joeri F.M. Denayer *

Vrije Universiteit Brussel, Brussels 1050, Belgium

ARTICLE INFO

Keywords:
CO_2 capture
Induction heating
Electrification
Adsorption

ABSTRACT

Electrification of chemical processes is one of the approaches designated to reach carbon neutrality in Europe by 2050. To take steps towards this goal, replacing traditional methods of heating with more advanced electrified methods is under investigation. In the present study, the fast thermal regeneration of composite sorbents was investigated under induction heating, as an alternative to traditional heating in Thermal Swing Adsorption processes. Extrudates of composite sorbents containing 13X zeolite and Fe_3O_4 as the main ingredients were prepared and subjected to heating quantification, equilibrium measurement, and dynamic ad/desorption experiments. From the heating quantification, it was deduced that the electric current in the induction coil has a direct impact on the specific rate of heat absorption with the maximum heat-absorption rate of 150 W per unit gram of Fe_3O_4 at 171 A. The equilibrium measurement of CO_2 and N_2 adsorption proved that the mass adsorption capacity of the hybrid material decreases as the content of Fe_3O_4 increases; however, due to the dense nature of Fe_3O_4, the content of 13X per unit volume of the sorbent with 20 wt% Fe_3O_4 (13X-IO20) is only 2% less than that of a sorbent with 10 wt% Fe_3O_4 (13X-IO10). Under the same electric current in the coil, the net amount of energy that the 13X-IO20 can absorb is almost twice as big as the one of 13X-IO10, while the maximum desorption rate of the 13X-IO20 was almost three times bigger than that of the 13X-IO10. By comparing the measured desorption rates with reported data in literature, it was found that at high coil currents the desorption rate is one order higher than the reported values.

1. Introduction

The European Green Deal was signed in 2019 (in line with the Paris agreement on climate change) to make Europe the world's first carbon–neutral continent by 2050 [1]. This deal includes a series of policies and legislation to control carbon emissions from different sources. Among these sources, a considerable portion of CO_2 is released by industrial activities, mainly from burning fossil fuels to provide thermal energy and as a by-product of various chemical processes. To effectively reduce the carbon footprint of fossil fuel-based thermal energy generation, when renewable electricity is widely available, advanced electrified methods of heating such as microwave, induction, and resistive heating can be applied. In particular, the CO_2 produced in a chemical process can be removed via an electrified carbon capture process.

Adsorption is one of the promising carbon capture technologies, as it offers a high separation factor and can create products with a high purity with a reasonable energy penalty [2]. The sorbents for such an adsorptive carbon capture have been widely studied in the last few decades and extensive data are available in the literature [3]. These sorbents can be categorized into microporous zeolites, activated carbonaceous materials, mesoporous silica/alumina, polymeric sorbents, and metal–organic frameworks. In many cases, functional groups such as amines or metal oxides were loaded into the porous structure of such adsorbents via one or a combination of techniques including wet impregnation [4], surface grafting [5], and chemical vapor deposition [6]. The incorporated functional groups can create a strong bond with CO_2 and enhance both adsorption capacity and affinity even under humid conditions.

The processes in which the sorbents have been tested for carbon capture can be divided into two main categories: Pressure/Vacuum Swing adsorption (P/VSA) and Temperature Swing Adsorption (TSA). These processes include at least two beds, where one bed adsorbs the CO_2 from the target gas stream; while concentrated CO_2 is obtained from the other either by pressure reduction (P/VSA) or by heating the bed (TSA). P/VSA is an electrified process in nature (the compressor and

* Corresponding author.
E-mail address: joeri.denayer@vub.be (J.F.M. Denayer).

https://doi.org/10.1016/j.cej.2021.133380
Received 26 August 2021; Received in revised form 25 October 2021; Accepted 31 October 2021
Available online 7 November 2021

Nomenclature

b	adsorption affinity parameter (1/bar)
C_p	heat capacity (J/kg K)
E	adsorption activation energy (J/mol)
m	mass (kg)
P	partial pressure (bar)
Q	heating rate (W)
q^*	equilibrium adsorption capacity (mol/kg)
q_s	saturation adsorption capacity (mol/kg)
R	universal gas constant 8.314 (J/mol K)
SAR	specific absorption rate (W/g)
T	temperature (K)
t	time (s)

Subscript

0	reference condition
1, 2	indexes for sites 1 and 2 of dual-site Langmuir model
ads	adsorbent
IO	iron oxide
tot	total
v	vial
w	water

Greek letters

χ	fitting parameter for correlating the temperature dependence of maximum adsorption capacity

vacuum pumps use electric energy) for which extensive research work is available in the literature [7–9]. A recent optimization study by Krishnamurthy *et al.* indicated that the VSA process can separate CO_2 from a binary mixture of 0.15/0.85 CO_2/N_2 by the energy consumption of about 1 MJ/ kg CO_2 with the constraints of 90% recovery, and 95% purity [10].

In contrast with P/VSA, the source of thermal energy in most of the commercial TSA processes is a fossil fuel. Though, electrical TSA processes have also been studied with the aim of developing an electrified process for carbon capture. To regenerate the adsorbent in these processes, the electricity converted to heat via three different technologies: Joule heating (Electric Swing Adsorption, ESA) [11,12], microwave heating (Microwave Swing Adsorption, MSA) [13], and induction heating (Magnetic Induction Swing Adsorption, MISA) [14].

One of the earliest studies on the ESA process was carried out in the late 20th century in Oak Ridge National Laboratory for CH_4/CO_2 separation [15]. In this process, the ohmic resistance of the adsorbents (which are usually made completely or partially of carbonaceous material) converts electricity to heat. The electric current must be distributed evenly along the bed, as the maldistribution of the electricity can cause a hot spot which is very unsafe when a carbonaceous material is available. This need for uniform connectivity along the bed makes the scale-up a challenge [16,17]. In contrast to ESA, in MSA and MISA the adsorbent does not need to be continuous along the bed, and can heat up remotely as far as the sorbent has the capability of getting hot under microwave irradiation or alternative magnetic induction. One of the earliest studies on heating the adsorption bed by microwaves in CO_2 separation was done in 1997 when a layered bed was applied to remove CO_2, acetone and water vapor from an air stream [18]. It was observed that adsorbed water on silica gel, 13X, and 5A zeolite, and adsorbed CO_2 on the 5A zeolite and a carbogenic molecular sieve were desorbed under microwave irradiation. Although both microwave and induction technologies were developed in the mid-20th century, induction heating technology has succeeded to find its way to large-scale heating processes sooner.

In induction heating, a high-frequency alternating magnetic field induces eddy currents inside the conductive materials. It also changes the direction of aligned domains of the magnetic materials. These two phenomena cause a rise in temperature either due to ohmic resistance or by magnetic dissipation. One of the earliest studies on induction heating of adsorbents was reported in 1994 [19]. In this study, the desorption of volatile organic compounds from activated carbon was done by induction heating. It was found that incorporating a susceptor such as graphite inside the adsorbent enhances the efficiency of heating. The first study on the use of this method for CO_2 desorption from an adsorbent was reported by Sadiq *et al.* in 2016 [14]. By developing a composite sorbent made of UiO-66 MOF and ferri-magnetic $MgFe_2O_4$ nanoparticles, it was possible to heat the sorbent under an alternating induced magnetic field. The regeneration of sorbent was done in 4 min, with a 100% release of CO_2 from the sorbent. In 2020, Sadiq *et al.* developed a composite sorbent made of $MgFe_2O_4$ and Mg-MOF-74, and performed breakthrough and regeneration experiments for 3 g of sorbent powder which was packed in a bed with a 1.5 cm diameter [20]. They calculated that by this method of heating, the specific energy of regeneration was 1.29 MJ/kg CO_2. In 2020, Lin *et al.* studied the pure CO_2 adsorption/desorption under induction heating by an amine doped mesoporous carbon in which superparamagnetic particles of Fe_3O_4 were used as the susceptor [21]. The desorption experiments were performed under two different conditions of a fixed target temperature and a constant current mode. The best-calculated energy efficiency was 79.2% with an energy consumption of 3.43 MJ/kg CO_2.

The results obtained in the above-mentioned works using lab-synthesized materials are promising; however, further explorations are needed on the use of induction heating as a feasible technology in adsorptive carbon capture when commercial materials such as 13X zeolite and Fe_3O_4 are used. Because both 13X zeolite and Fe_3O_4 are widely available, two types of sorbents pellets containing different amounts of Fe_3O_4 particles were extruded in this work. Equilibrium isotherms of CO_2 and N_2 on both samples were measured, and the mass and volumetric sorption capacity reduction were analyzed. To shed light on the potentials of the induction heating for sorbent regeneration, the specific absorption rate of energy for both samples was assessed, and finally, the dynamic of CO_2 desorption under induction heating was investigated.

2. Experimental section

2.1. Sorbent preparation and characterization

The materials used to prepare the adsorbent pellets are 13X-AP zeolite powder (UOP), Fe_3O_4 (IO) powder, bentonite, and polyvinyl alcohol. The adsorbent was shaped into extrudates according to the method developed by Mirmohammadi and Shams [22]. The 13X and bentonite powder was dispersed in water to form a paste. Subsequently, the paste was left in a convection oven overnight to dry. The obtained solid was crushed and blended with desired amounts of Fe_3O_4 powder. In the next step, a solution of polyvinyl alcohol in water was added dropwise, and the mixture was vigorously kneaded until an appropriate paste was obtained. The paste then was transferred into a handheld extruder and was shaped into 1 mm diameter extrudate strings (Fig. 1). The resulting strings were left to dry overnight at ambient temperature, and were crushed into 2 to 4 mm pellets; finally, the samples calcined at 700 °C. In all of the samples, the amount of Fe_3O_4 was chosen in such a way to have samples with the mass fractions of 10 and 20 % of Fe_3O_4. These composite adsorbents were named 13X-IO10 and 13X-IO20 respectively. The Ar-porosimetry (Autosorb-1, Quantachrome instruments device at 87 K) was used to estimate surface area, pore size distribution, and pore volume of the sorbents [23,24]. The pellet density was determined by measuring the apparent mass of the samples in water. The details of the measuring method are provided in the supplementary information (SI).

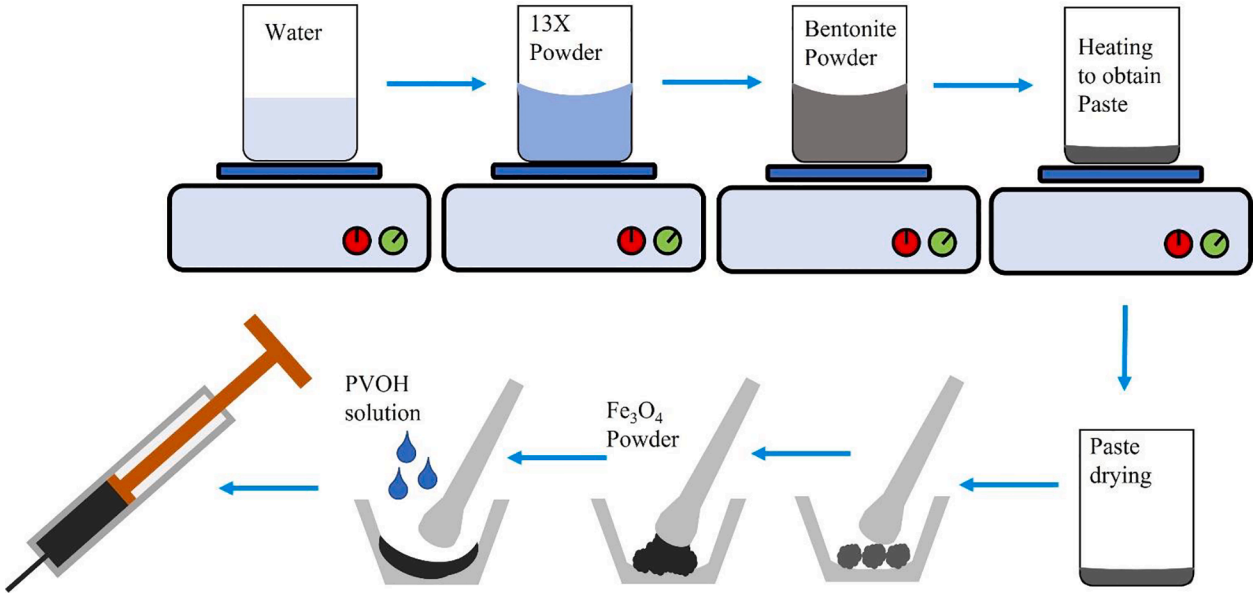

Fig. 1. Schematical representation of sorbent shaping.

3. Induction heating of the samples

An induction heater (AMBRELL, 8310) with a round coil (7 cm length, 2.8 cm ID, 3.8 OD, 8 turns) heated the adsorbents. To quantify the amount of generated heat at different currents of the induction heater, 1.00 g of the shaped samples was crushed and dispersed in 8.86 g of water in a glass vial. The suspension was heated under different coil currents. During the heating, the suspension was mixed with a 4 mm polymeric blade and the temperature of the suspension was continuously measured using a fiber-optic (FO) temperature sensor (OPTOCON, TS5). The initial slopes of the measured temperature profiles were used to calculate the rate of generated heat in different samples (see Eq. (1) and (2)).

$$\left.\frac{\mathbf{d}T}{\mathbf{d}t}\right|_{t=0} = \frac{Q}{(mC_P)_{\text{tot}}} \tag{1}$$

$$(mC_P)_{\text{tot}} = (mC_P)_{\text{w}} + (mC_P)_{\text{v}} + (mC_P)_{\text{ads}} \tag{2}$$

Later, this generated heat was used to calculate the specific absorption rate (SAR) using Eq. (3).

$$SAR = \frac{Q}{m_{\text{IO}}} \tag{3}$$

To calibrate the total heat capacity of the system, the same system was heated by a resistive heater at different specific powers. Since the applied powers were known during these experiments, the measured initial temperature gradients were used to experimentally estimate the overall heat capacity of the system.

3.1. Equilibrium and dynamic measurements

The CO_2 isotherms were measured for both adsorbents (13X-IO10

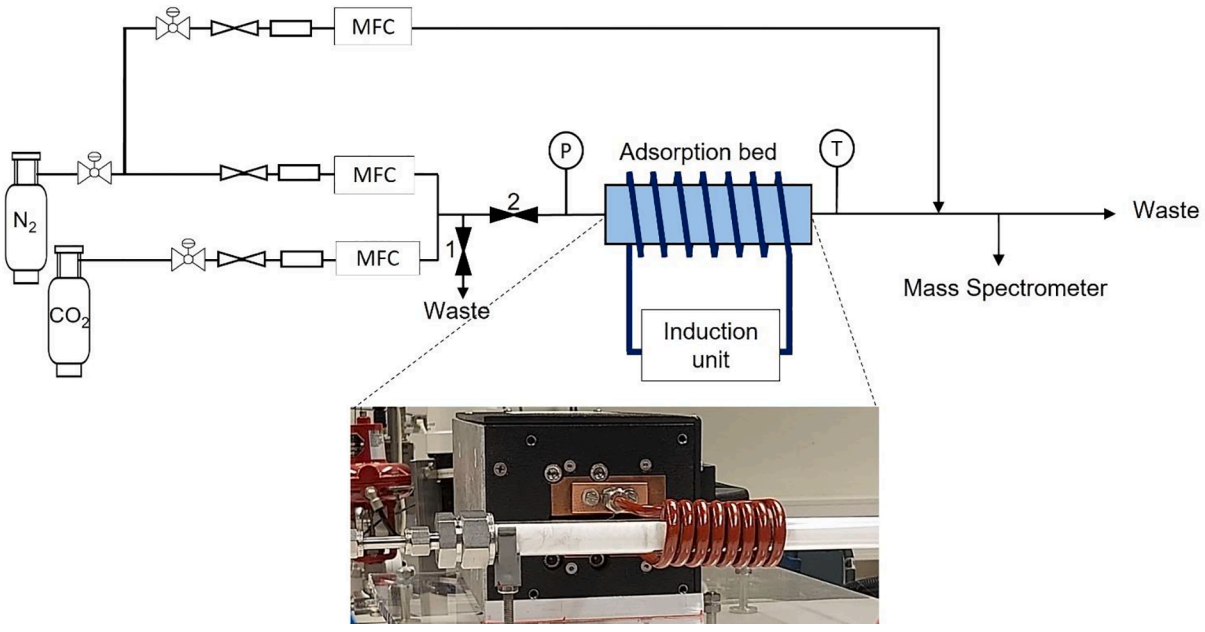

Fig. 2. The scheme of the setup and a picture of the column and induction coil that is used for measuring adsorption and desorption dynamics.

and 13X-IO20) at 303, 333, and 363 K in the pressure range of 0 to 1 bar by Autosorb-1 (Quantachrome Instruments, Odelzhausen, Germany). N_2 isotherms were measured by the static volumetric method using an HPA-100 device (VTI corporation) at 283, 303, and 333 K in the pressure range of 0 to 6 bar. Prior to the isotherm measurement, the samples were outgassed at 623 K for 3 h.

The CO_2 dynamic adsorption and desorption experiments were carried out using an in-house built lab setup (Fig. 2). A quartz tube was used as the column since metallic ones tend to heat up under induction. The length of the quartz tube was chosen in such a way that the metallic fittings and connectors were not affected by the magnetic field of the induction heater coil. Two pieces of PTFE rods with an axial hole (2 mm diameter) through them were put at both sides of the sorbent bed to reduce the dead volume. The holes at one side (in touch with adsorbent) of the rods were conical to help with the uniformity of the flow in the adsorbent bed. More information about the column packed with extrudates is presented in Table 1. A pressure transmitter was installed at the inlet of the column, and a FO temperature sensor was installed at the outlet of the bed in such a way that the tip of the FO was touching the adsorbents in the bed. The feed composition was adjusted by thermal mass flow controllers (Bronkhorst). A Thermostar GSD 300 T3 mass spectrometer was used to detect the composition of the column effluent.

Before each regeneration experiment, breakthrough experiments were performed to have the composite sorbents saturated under identical conditions. All dynamic experiments were performed at atmospheric pressure, while the ambient temperature was kept at 294 ± 1 K. The flow rates of gases in the breakthrough experiments were 170 NmL/min of N_2 and 30 NmL/min of CO_2. In the regeneration test, the bed was purged with 30 NmL/min of N_2. To estimate the flow of desorbed CO_2, the effluent was diluted with a constant stream of N_2 (50 NmL/min) before sending the mixture to the MS. Several experiments were performed to study the effect of the induction strength and the susceptor content on the desorption rate of CO_2.

3.2. Results and discussions

The results of Ar-porosimetry and the pellet density measurement are presented in the SI. The results described here consist of the assessment of heat absorption under induction by the adsorbents, the evaluation of equilibrium isotherms of CO_2 and N_2, and the analysis of the dynamic data of the adsorption and desorption.

3.3. Heating quantification

The overall heat capacity of the cell containing water and the samples was measured to be 50 J/K. The details of the overall heat capacity measurements are presented in the SI. The heat absorption of the samples was measured under different magnetic field strengths. Since the strength of a magnetic field is a function of the electric current in the coil, different magnetic fields were generated by setting the electric current (49.4–171.0 A). The SAR for both samples at different currents was calculated based on the net mass of IO in each sample (Table 2). The trends of the changes for both samples are similar, and the SARs are in the same order in each current. However, since the content of IO particles in 13X-IO20 is two times higher than the one in 13X-IO10, the net generated heat in it is almost two times higher (Table 2).

Table 1
Properties of the adsorption column.

Column packed with	13X-IO10	13X-IO20
Column ID, cm	1.61.9	
Column OD, cm		
Adsorbent bed length, cm	5.7	
Adsorbent Mass, g	5.6	6.1

Table 2
The specific absorption rate of energy of both samples at different currents.

Applied current (A)	Frequency (kHz)	SAR (W/g) 13X-IO10	13X-IO20
49.4	250	9.5	8.1
74.1	250	24.4	18.2
100.7	248	58.1	46.7
171.0	248	149.7	137.9

3.4. Adsorption equilibrium isotherm

Fig. 3(a-d) display the equilibrium isotherm data of pure CO_2 and N_2 on 13X-IO10 and 13X-IO20 materials. The obtained experimental data were regressed with the Dual Site Langmuir (DSL) model (Eq. (4) to (6)) to estimate the pure component isotherm parameters (Table 3).

$$q^* = q_{s1}\frac{b_1 P}{1+b_1 P} + q_{s2}\frac{b_2 P}{1+b_2 P} \tag{4}$$

$$q_s = q_{s0} exp\left[\chi\left(1-\frac{T}{T_0}\right)\right] \tag{5}$$

$$b = b_0 exp\left[-\frac{E}{RT_0}\left(1-\frac{T_0}{T}\right)\right] \tag{6}$$

Since the only difference between the two sorbent samples is the content of Fe_3O_4, the differences between their capacities are attributed to different contents of 13X particles per unit mass of the composite sorbent. This deduction is confirmed when the adsorption isotherms of CO_2 for both samples at 303 K per unit mass of used 13X are compared with the isotherm of CO_2 for the 13X-AP powder (Fig. 4).

The active 13X zeolite mass content of 13X-IO20 is 89% of its content in 13X-IO10. However, it must not be overlooked that a higher content of IO causes a denser composite sorbent. The densities of the extrudates were 886 and 971 kg/m^3 for the 13X-IO10 and 13X-IO20 respectively. Based on these densities, the ratio of 13X content per unit volume of 13X-IO20 is 98% of the 13X content per unit volume of 13X-IO10. Thus, the adsorption capacity of the same bed of 13X-IO20 is just 2 % lower than that of the 13X-IO10. The density of the composite sorbents can be roughly estimated by the arithmetic average of a pellet density without IO and the density of IO itself using Eq. (7). Then, the relative volumetric fraction of 13X in pellets can be calculated using Eq. (8).

$$\rho_{comp} = \frac{1}{\left(\frac{1-X_{IO}}{\rho_p}+\frac{X_{IO}}{\rho_{IO}}\right)} \tag{7}$$

$$13X_{VF}\% = \frac{\rho_{comp}(1-X_{IO})}{\rho_p} * 100 \tag{8}$$

Fig. 5 shows the 13X relative volumetric fraction of the sorbents and the sorbent density as a function of the IO mass fraction in the composite sorbent. Given the fact that the IO density is 5170 kg/m^3 (significantly higher than that of 13X zeolite), the density of the composite sorbent increases as the content of IO increases. The relative volumetric fraction of 13X varies between 86 and 98%. This is beneficial from a practical point of view since by losing less than 15% of volumetric capacity, a large amount of IO can be embedded into the bed, which allows the regeneration of the bed in a much shorter time than in the traditional TSA (as discussed in the next section).

3.5. Adsorption and desorption dynamics

The breakthrough curves (see SI) as well as the desorption curves of CO_2 for the composite sorbents, along with the gas temperature at the outlet of the bed were recorded as a function of time (Fig. 6 (a-d)). To evaluate the effect of IO content and the strength of different magnetic

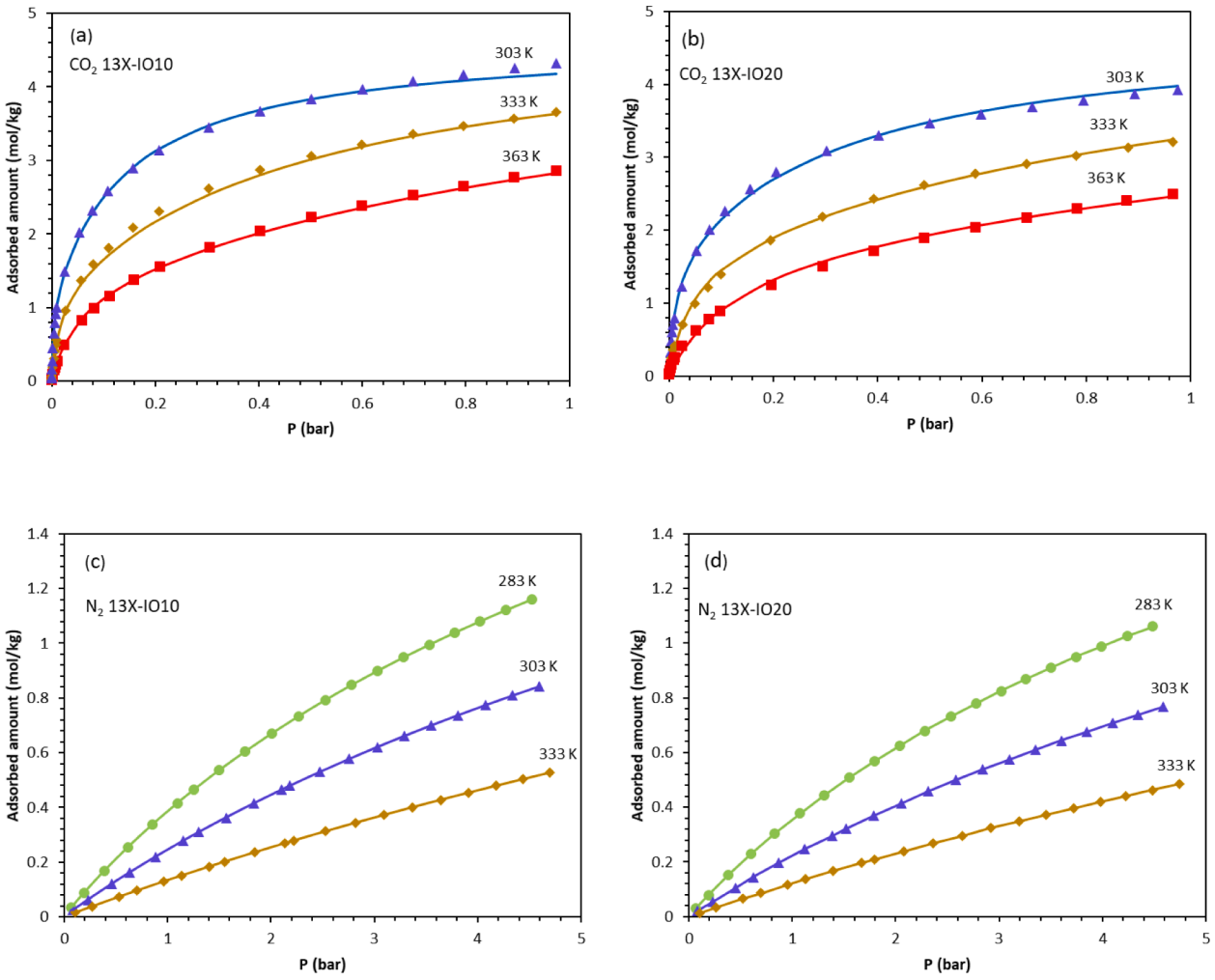

Fig. 3. Adsorption equilibrium isotherm of CO_2/13X-IO10 (a), CO_2/13X-IO20 (b), N_2/13X-IO10 (c), and N_2/13X-IO20 (d) pairs. Points: experimental data; lines: DSL model.

Table 3
Fitting parameters of the DSL model for adsorption isotherm of CO_2 and N_2 on both composite sorbents

		CO_2		N_2	
		13X-IO10	13X-IO20	13X-IO10	13X-IO20
Site I	q_{s0} (mol/kg)	1.05	1.48	0.083	0.047
	χ	−0.9	−0.81	4.4	10.4
	b_0 (1/bar)	509	149.5	0.675	0.88
	E (kJ/mol)	41.1	37.1	22.5	22.5
Site II	q_{s0} (mol/kg)	3.5	3.16	2.855	2.578
	χ	−0.5	−1.34	0.26	0.26
	b_0 (1/bar)	11.4	5.1	0.1052	0.1109
	E (kJ/mol)	35.0	37.6	16.1	16.1

fields, desorption experiments were performed at four different currents (49.4, 74.1, 100.7, and 171.0 A) for each sorbent. The reproducibility of the data was checked by repeating the same experiment for both samples at 100.7 A (See Fig. S8). Right after turning on the induction heater, without any delay the temperature rise was recorded (the tip of the FO temperature sensor was placed at the bed outlet) (Fig. 6 (b,d)); and it is while there is a time delay of approximately 4 s before measuring any change in effluent composition by the mass spectrometer (Fig. 6(a,c)) due to the distance between bed outlet and MS probe (Fig. 2). All of the measured temperature profiles contain an initial steep rise, then a moderate rise, and finally, a slow rise to a final temperature. The heat absorbed by the IO particles first causes the sorbent temperature to rise.

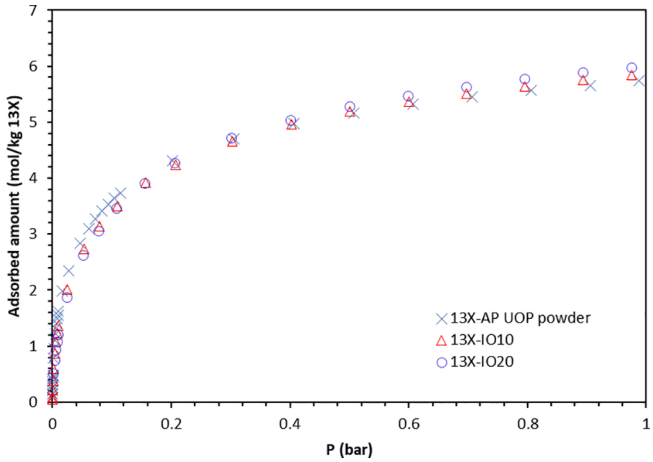

Fig. 4. CO_2 isotherms at 303 K for both samples normalized per unit mass of 13X zeolite.

Since the adsorption equilibrium is a function of temperature, gradually the desorption starts. As the desorption enthalpy and heat loss to ambient consume the absorbed heat, the slope of temperature rise reduces. When the desorption rate is not significant anymore, the temperature rises again to achieve thermal equilibrium.

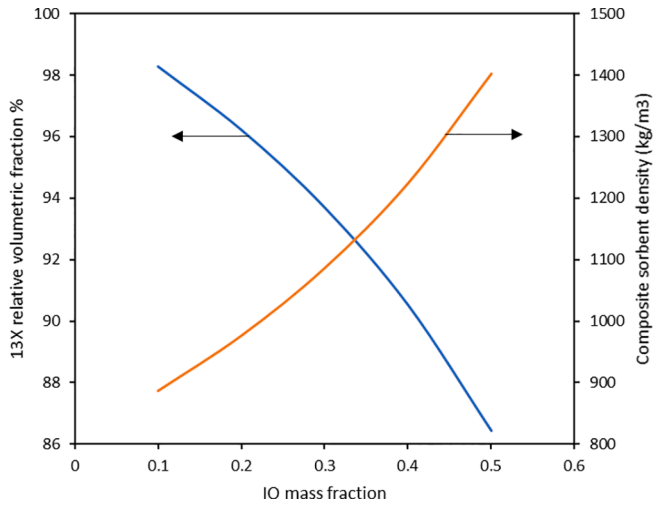

Fig. 5. Relative volumetric fraction and the sorbent density versus IO content.

As the applied current in the induction heating gets larger, the desorption takes place in a shorter time and causes a higher fraction of CO_2 in the outlet stream (Fig. 6). For both samples, at 49.4 A the desorption time is of the order of hours, a common regeneration time in a traditional TSA process, while at 171.0 A it is of the order of minutes. Such a fast sorbent regeneration was reported by Gao et al. for a thin film of polyamine nano-gel coated on a carbon paper [25], or for the sorbent which was coated on the surface of a heat exchanger [26]. To our knowledge, the desorption rate of 461.4 mg/g min at 171.0 A for 13X-IO20 is one of the largest desorption rates ever reported for a pelletized sorbent (Table 4). The average desorption rate of 13X-IO20 at 171.0 A is one order higher than the reported desorption rate in the literature (Table 5). This confirms the great potential that contactless methods of heating such as induction offer to the chemical industry.

By comparing the maximum desorption rate of both samples, it is seen that the maximum desorption rate of 13X-IO20 is almost three times bigger than the one of 13X-IO10, while its IO content is just two times bigger than that of the 13X-IO10 material. This increase in desorption rate with IO content is related to the mechanisms of energy absorption. Part of this energy warms the sorbent, some of it is consumed as the desorption enthalpy, and the rest is dissipated into the gas stream. Since the thermal conductivity of zeolites is low, a higher

Table 4
Maximum desorption rate for both samples at different currents

Adsorbent	Maximum desorption rate (mg/g min) 171.0 A	100.7 A	74.1 A	49.4 A
13X-IO10	156.8	38.3	17.5	5.7
13X-IO20	461.4	108.1	45.9	14.3

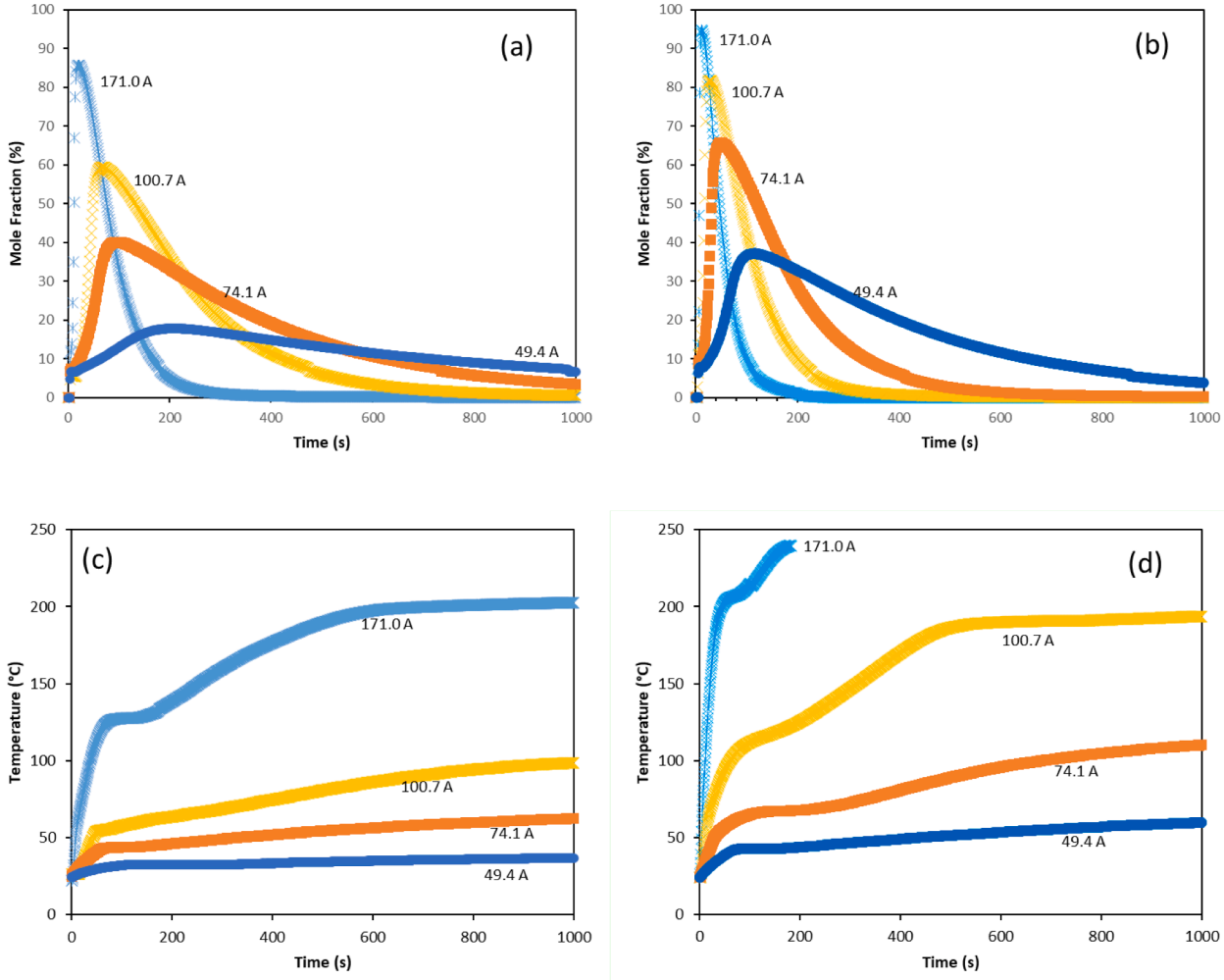

Fig. 6. CO_2 desorption curves from a column packed with (a) 13X-IO10 and (b) 13X-IO20, and outlet temperature of the bed containing (c) 13X-IO10 and (d) 13X-IO20. (At 171.0 A for 13X-IO20 the heating was stopped to prevent damaging the FO).

Table 5
Comparison of average desorption rates with reported data in the literature

Average desorption rate (95 % desorption)[a] (mg/g min)					
Adsorbent	171.0 A	100.7 A	74.1 A	49.4 A	Reference
13X-IO10	45.2	12.4	4.4	Less than 1.3	Present study
13X-IO20	103.0	33.5	15.2	4.0	Present study
Process type	Adsorbent	Average desorption rate[c](mg/g min)			
TCSD[b]	Amine loaded silica	3.67	[27]		
TCSD	Amine loaded MOF	7.39	[28]		
TCSD	Amine loaded carbon	4.32	[29]		
Steam stripping	Amine loaded silica	10.16	[30]		
Steam stripping	Amine loaded silica	9.14	[31]		
Steam stripping	Amine loaded silica	12.80	[32]		
TVSA	13X-APG	2.03	[33]		
Rotating bed TVSA	Amine-containing nano-gel particles	10.37	[34]		

[a] The 95 % desorption rate was calculated by integrating the desorption rate over time to reach 95 % desorption of the initially adsorbed amount
[b] Temperature concentration swing desorption
[c] The average desorption rate was calculated by dividing the total desorbed amount by the time of desorption.

portion of absorbed energy is consumed to warm the sorbent and supply the heat of adsorption at higher heating intensity.

4. Conclusion

In the present study, two composite sorbents that can heat up under induction were prepared in extrudate form, using commercially available 13X and Fe_3O_4. The measurement of the specific absorption rate of the energy indicated that the net amount of generated heat inside the sorbents is a direct function of electric current and IO content in which the latter has a dual effect: on one hand, it enhances the regeneration efficiency; on the other hand, it lowers adsorption capacity due to the lower amount of active zeolite per unit mass of the sorbent. However, it was deduced from the density measurement of the composite material that increasing the IO content makes the sorbent denser and does not result in a large sacrifice in the volumetric capacity. The evaluated desorption dynamics showed that at a high energy absorption rate, the regeneration time could be reduced into a period as short as one minute, which is at least one order lower than the regeneration time of a normal TSA process. Such a short regeneration time will effectively reduce the amount of adsorbent inventory. It is worth mentioning that the use of inductive heating allows for localized and precise temperature control. In general, this study revealed the potentials of induction heating and the commercial materials for the development of an electrified adsorptive carbon capture process.

Declaration of Competing Interest

The authors declare that they have no known competing financial interests or personal relationships that could have appeared to influence the work reported in this paper.

Acknowledgments

The authors would like to acknowledge VLAIO for the financial support (HBC.2019.0109).

Appendix A. Supplementary data

Supplementary data to this article can be found online at https://doi.org/10.1016/j.cej.2021.133380.

References

[1] A European Green Deal Striving to be the first climate-neutral continent, (2019). https://ec.europa.eu/info/strategy/priorities-2019-2024/european-green-deal_en#documents.
[2] M. Bui, C.S. Adjiman, A. Bardow, E.J. Anthony, A. Boston, S. Brown, P.S. Fennell, S. Fuss, A. Galindo, L.A. Hackett, J.P. Hallett, H.J. Herzog, G. Jackson, J. Kemper, S. Krevor, G.C. Maitland, M. Matuszewski, I.S. Metcalfe, C. Petit, G. Puxty, J. Reimer, D.M. Reiner, E.S. Rubin, S.A. Scott, N. Shah, B. Smit, J.P.M. Trusler, P. Webley, J. Wilcox, N. Mac Dowell, Carbon capture and storage (CCS): the way forward, Energy Environ. Sci. 11 (5) (2018) 1062–1176, https://doi.org/10.1039/C7EE02342A.
[3] A. Samanta, A.N. Zhao, G.K.H. Shimizu, P. Sarkar, R. Gupta, Post-combustion co2 capture using solid sorbents: A review, Ind. Eng. Chem. Res. 51 (4) (2012) 1438–1463, https://doi.org/10.1021/ie200686q.
[4] H. Thakkar, S. Eastman, A. Al-Mamoori, A. Hajari, A.A. Rownaghi, F. Rezaei, Formulation of aminosilica adsorbents into 3d-printed monoliths and evaluation of their co2 capture performance, ACS Appl. Mater. Interfaces. 9 (8) (2017) 7489–7498, https://doi.org/10.1021/acsami.6b1673210.1021/acsami.6b16732.s001.
[5] M. Gholami, M.R. Talaie, S.F. Aghamiri, CO2 adsorption on amine functionalized MCM-41: effect of bi-modal porous structure, J. Taiwan Inst. Chem. Eng. 59 (2016) 205–209, https://doi.org/10.1016/j.jtice.2015.07.021.
[6] W. Zhu, Y. Yao, Y. Zhang, H. Jiang, Z. Wang, W. Chen, Y. Xue, Preparation of an amine-modified cellulose nanocrystal aerogel by chemical vapor deposition and its application in co2 capture, Ind. Eng. Chem. Res. 59 (38) (2020) 16660–16668, https://doi.org/10.1021/acs.iecr.0c02687.
[7] A. Al-Mamoori, A. Krishnamurthy, A.A. Rownaghi, F. Rezaei, Carbon capture and utilization update, Energy Technol. 5 (2017) 834–849, https://doi.org/10.1002/ente.201600747.
[8] C. Dhoke, S. Cloete, S. Krishnamurthy, H. Seo, I. Luz, M. Soukri, Y.-k. Park, R. Blom, S. Amini, A. Zaabout, Sorbents screening for post-combustion CO2 capture via combined temperature and pressure swing adsorption, Chem. Eng. J. 380 (2020) 122201, https://doi.org/10.1016/j.cej.2019.122201.
[9] S. Krishnamurthy, V.R. Rao, S. Guntuka, P. Sharratt, R. Haghpanah, A. Rajendran, M. Amanullah, I.A. Karimi, S. Farooq, CO2 capture from dry flue gas by vacuum swing adsorption: a pilot plant study, AIChE J. 60 (5) (2014) 1830–1842, https://doi.org/10.1002/aic.v60.510.1002/aic.14435.
[10] S. Krishnamurthy, J. Boon, C. Grande, A. Lind, R. Blom, R. Boer, H. Willemsen, G. Scheemaker, Screening supported amine sorbents in the context of post-combustion carbon capture by vacuum swing adsorption, Chemie Ing. Tech. 93 (6) (2021) 929–940.
[11] C.A. Grande, A.E. Rodrigues, Electric swing adsorption for CO2 removal from flue gases, Int. J. Greenh. Gas Control. 2 (2008) 194–202, https://doi.org/10.1016/S1750-5836(07)00116-8.
[12] B. Verougstraete, A. Martín-Calvo, S. Van der Perre, G. Baron, V. Finsy, J.F. M. Denayer, A new honeycomb carbon monolith for CO2 capture by rapid temperature swing adsorption using steam regeneration, Chem. Eng. J. 383 (2020) 123075, https://doi.org/10.1016/j.cej.2019.123075.
[13] T. Chronopoulos, Y. Fernandez-Diez, M.M. Maroto-Valer, R. Ocone, D.A. Reay, CO2 desorption via microwave heating for post-combustion carbon capture, Microporous Mesoporous Mater. 197 (2014) 288–290, https://doi.org/10.1016/j.micromeso.2014.06.032.
[14] M.M. Sadiq, H. Li, A.J. Hill, P. Falcaro, M.R. Hill, K. Suzuki, Magnetic induction swing adsorption: an energy efficient route to porous adsorbent regeneration, Chem. Mater. 28 (17) (2016) 6219–6226, https://doi.org/10.1021/acs.chemmater.6b0240910.1021/acs.chemmater.6b02409.s001.
[15] T.D. Burchell, R.R. Judkins, Passive CO2 removal using a carbon fiber composite molecular sieve, Energy Convers. Manag. 37 (1996) 947–954, https://doi.org/10.1016/0196-8904(95)00282-0.
[16] N. Vanden Haute, CARBON-BASED MONOLITHS FOR CARBON DIOXIDE CAPTURE VIA ELECTRICAL SWING ADSORPTION: SYNTHESIS, CHARACTERISATION AND MODELLING, Vrije Universiteit Brussel, 2020.
[17] C.A. Grande, R.P.L. Ribeiro, E.L.G. Oliveira, A.E. Rodrigues, Electric swing adsorption as emerging CO2 capture technique, Energy Procedia. 1 (2009) 1219–1225, https://doi.org/10.1016/j.egypro.2009.01.160.
[18] J.E. Atwater, J.T. Holtsnider, R.R. Wheeler, B. Luna, Microwave-powered thermal regeneration of sorbents for CO2, Water Vapor and Trace Organic Contaminants (1997), https://doi.org/10.4271/972430.
[19] P. Mocho, P. Le Cloirec, Regeneration of granular activated carbon by inductive heating - Application in the elimination and recycling of air-born solvents, in: S. Vigneron, J. Hermia, J.B.T.-S, in: E.S. Chaouki (Ed.), Charact, Elsevier, Control

Odours VOC Process Ind., 1994, pp. 251–259, https://doi.org/https://doi.org/10.1016/S0166-1116(08)72059-4.
[20] M.M. Sadiq, K. Konstas, P. Falcaro, A.J. Hill, K. Suzuki, M.R. Hill, Engineered porous nanocomposites that deliver remarkably low carbon capture energy costs, Cell Reports Phys. Sci. 1 (2020), 100070, https://doi.org/10.1016/j.xcrp.2020.100070.
[21] X. Lin, B. Shao, J. Zhu, F. Pan, J. Hu, M. Wang, H. Liu, In situ electromagnetic induction heating for co2 temperature swing adsorption on magnetic fe3o4/n-doped porous carbon, Energy & Fuels. 34 (11) (2020) 14439–14446, https://doi.org/10.1021/acs.energyfuels.0c0269910.1021/acs.energyfuels.0c02699.s001.
[22] K. Shams, S.J. Mirmohammadi, Preparation of 5A zeolite monolith granular extrudates using kaolin: Investigation of the effect of binder on sieving/adsorption properties using a mixture of linear and branched paraffin hydrocarbons, Microporous Mesoporous Mater. 106 (2007) 268–277, https://doi.org/10.1016/j.micromeso.2007.03.007.
[23] M. Thommes, Physical adsorption characterization of nanoporous materials, Chemie Ing. Tech. 82 (2010) 1059–1073, https://doi.org/10.1002/cite.201000064.
[24] M. Thommes, K.A. Cychosz, Physical adsorption characterization of nanoporous materials: progress and challenges, Adsorption. 20 (2-3) (2014) 233–250, https://doi.org/10.1007/s10450-014-9606-z.
[25] J. Gao, Y. Liu, Y. Terayama, K. Katafuchi, Y. Hoshino, G. Inoue, Polyamine nanogel particles spray-coated on carbon paper for efficient CO2 capture in a milli-channel reactor, Chem. Eng. J. 401 (2020), 126059, https://doi.org/10.1016/j.cej.2020.126059.
[26] F. Esmaeili, M. Hojjat, J.F.M. Denayer, M. Gholami, CO2 Capture on an adsorbent-coated finned tube heat exchanger: effect of the adsorbent thickness, Ind. Eng. Chem. Res. 60 (12) (2021) 4677–4681, https://doi.org/10.1021/acs.iecr.0c06171.
[27] A. Goeppert, H. Zhang, M. Czaun, R.B. May, G.K.S. Prakash, G.A. Olah, S. R. Narayanan, Easily regenerable solid adsorbents based on polyamines for carbon dioxide capture from the air, ChemSusChem. 7 (2014) 1386–1397, https://doi.org/10.1002/cssc.201301114.
[28] T.M. McDonald, W.R. Lee, J.A. Mason, B.M. Wiers, C.S. Hong, J.R. Long, Capture of carbon dioxide from air and flue gas in the alkylamine-appended metal-organic framework mmen-Mg2(dobpdc), J. Am. Chem. Soc. 134 (16) (2012) 7056–7065, https://doi.org/10.1021/ja300034j.
[29] J. Wang, H. Huang, M. Wang, L. Yao, W. Qiao, D. Long, L. Ling, Direct capture of low-concentration co2 on mesoporous carbon-supported solid amine adsorbents at ambient temperature, Ind. Eng. Chem. Res. 54 (19) (2015) 5319–5327, https://doi.org/10.1021/acs.iecr.5b01060.
[30] N.K. Sandhu, D. Pudasainee, P. Sarkar, R. Gupta, Steam regeneration of polyethylenimine-impregnated silica sorbent for postcombustion co2 capture: a multicyclic study, Ind. Eng. Chem. Res. 55 (7) (2016) 2210–2220, https://doi.org/10.1021/acs.iecr.5b0474110.1021/acs.iecr.5b04741.s001.
[31] W. Li, S. Choi, J.H. Drese, M. Hornbostel, G. Krishnan, P.M. Eisenberger, C. W. Jones, Steam-stripping for regeneration of supported amine-based co2 adsorbents, ChemSusChem. 3 (2010) 899–903, https://doi.org/10.1002/cssc.201000131.
[32] S. Hammache, J.S. Hoffman, M.L. Gray, D.J. Fauth, B.H. Howard, H.W. Pennline, Comprehensive study of the impact of steam on polyethyleneimine on silica for co2 capture, Energy & Fuels. 27 (11) (2013) 6899–6905, https://doi.org/10.1021/ef401562w.
[33] L. Wang, Z. Liu, P. Li, J. Yu, A.E. Rodrigues, Experimental and modeling investigation on post-combustion carbon dioxide capture using zeolite 13X-APG by hybrid VTSA process, Chem. Eng. J. 197 (2012) 151–161, https://doi.org/10.1016/j.cej.2012.05.017.
[34] J. Gao, Y. Liu, Y.U. Hoshino, G. Inoue, Amine-containing nanogel particles supported on porous carriers for enhanced carbon dioxide capture, Appl. Energy. 253 (2019) 113567, https://doi.org/10.1016/j.apenergy.2019.113567.